

1 **IL-17A promotes epithelial cell IL-33 production during nematode lung**
2 **migration**

3 Jesuthas Ajendra^{1,2*}, Stella Pearson¹, James E. Parkinson¹, Brian H.K. Chan¹, Henry J.
4 McSorley³, Tara E. Sutherland^{1,3}, Judith E. Allen^{1*}

5 ¹Lydia Becker Institute of Immunology and Inflammation, Wellcome Trust Centre of Cell
6 Matrix Research, School of Biological Sciences, Faculty of Biology, Medicine and Health,
7 University of Manchester, Manchester, United Kingdom

8 ²Institute for Medical Microbiology, Immunology and Parasitology, University Hospital
9 Bonn, Bonn, Germany

10 ³Division of Cell Signalling and Immunology, School of Life Sciences, University of Dundee,
11 Dundee, United Kingdom

12 ⁴School of Medicine, Medical Sciences and Dentistry, Institute of Medical Sciences,
13 University of Aberdeen, Aberdeen, United Kingdom

14 *communicating authors

15

16 **Abstract**

17 The early migratory phase of pulmonary helminth infections is characterized by tissue injury
18 leading to the release of the alarmin IL-33 and subsequent induction of type 2 immune
19 responses. We recently described a role for IL-17A, through regulation of IFN γ , as an important
20 inducer of type 2 responses during infection with the lung-migrating rodent nematode
21 *Nippostrongylus brasiliensis*. Here, we aimed to investigate the interaction between IL-17A
22 and IL-33 during the early lung migratory stages of *N. brasiliensis* infection. In this brief report,
23 we demonstrate that deficiency of IL-17A leads to impaired IL-33 expression and secretion
24 early in infection, independent of IL-17A suppression of IFN γ . Impaired IL-33 production was
25 evident in lung epithelial cells, but not innate immune cells. Therefore, our results demonstrate
26 that IL-17A can drive IL-33 during helminth infection, highlighting an additional mechanism
27 through which IL-17A can regulate pulmonary type 2 immunity.

28

29 **Introduction**

30 Interleukin-33 (IL-33) belongs to the IL-1 cytokine family and plays a key role in innate and
31 adaptive immunity. IL-33 signals via the ST2 receptor, which is expressed on many different
32 cell types including eosinophils, group 2 innate lymphoid cells (ILC2) and Th2 cells¹. The
33 expression of ST2 on cell types closely associated with type 2 immunity and evidence that
34 IL-33 is a potent inducer of type 2 responses makes the IL-33/ST2 axis a therapeutic target in
35 type 2 mediated diseases. However, IL-33 is implicated more broadly in the maintenance of
36 tissue homeostasis, and has roles in protection against microbial infection and regulatory T cell
37 (Treg) expansion². In contrast to most other cytokines, IL-33 is usually released during cellular
38 necrosis, underpinning its role as an “alarmin” cytokine³. However, studies have also
39 demonstrated IL-33 release by cells of the airway epithelium including alveolar epithelial type
40 II (ATII) cells after infection with *Strongyloides venezuelensis* and administration of *Alternaria*
41 *alternata*, respectively^{4,5}.

42 The proinflammatory cytokine IL-17A is typically associated with host protection against
43 fungal and bacterial infections⁶. However, using a model of infection with the lung-migrating
44 nematode *Nippostrongylus brasiliensis* (*Nb*), we recently demonstrated that IL-17A is also
45 necessary to mount a pulmonary type 2 response^{7,8}. In this helminth setting, IL-17A from innate
46 $\gamma\delta$ T cells exerts a suppressive effect on IFN γ release by multiple cell types early during
47 infection⁷. This inhibition of IFN γ allows development of the adaptive pulmonary Th2
48 response. However, existing data on the interaction between IL-17A and IL-33⁹⁻¹² suggests the
49 possibility that innate IL-17A during *Nb* infection may function beyond its ability to suppress
50 IFN γ . In a neonatal mouse model of influenza, infection-induced IL-17A was associated with
51 increased IL-33 production by lung epithelial cells, subsequently generating a local type 2
52 immune response⁹. Similarly, mice lacking IL-17A exhibit decreased IL-33 in visceral adipose
53 tissue, leading to reduced Treg expansion and failure to regulate thermogenesis¹⁰. In both these
54 studies, as in lung *Nb* infection, the source of IL-17A is $\gamma\delta$ T cells^{7,8}. IL-17A-induced IL-33
55 also promotes type 2 immunity during atopic dermatitis with the IL-17A source being ILC3s¹¹.
56 Of note, during pulmonary *Aspergillus fumigatus* infection, IL-33 negatively regulates IL-17A
57 production¹², demonstrating cross-regulation between these two cytokines. During *Nb*
58 infection, we have shown IL-17A to be a driver of type 2 immunity^{7,8}, but Hung et al. have
59 demonstrated a pivotal role for IL-33 in the type 2 response in *Nb* infection¹³. Given the existing
60 literature on the interactions between IL-17A and IL-33 described above, we felt it essential to
61 investigate the relationship of these two cytokines during the lung-migrating phase of *Nb*
62 infection.

63 In this brief report we describe IL-17A stimulation of IL-33 release by the lung epithelium
64 during the early phase of *Nb* infection. However, this effect was independent of the IFN γ -
65 suppressing function of IL-17A. Furthermore, IL-17A-induced neutrophilia and the associated
66 lung damage was not the driver for IL-33 production. Together, our data demonstrate that IL-
67 17A acts as an upstream regulator of type 2 immune responses in the lung through two distinct
68 pathways; IFN γ -suppression and IL-33-secretion.

70 **Material & Methods**

71 **Mice**

72 C57BL/6 J mice were obtained from Charles River. C57BL/6 *Il17a*^{Cre}*Rosa26*^{eYFP} mice were
73 originally provided by Dr Brigitta Stockinger¹⁴. C57BL/6 *Il17a*^{Cre}*Rosa26*^{eYFP} homozygote mice
74 are IL-17A-deficient and described here as *Il17a*-KO. Male and female mice were age- and
75 sex-matched and housed in individually ventilated cages. Experimental mice were not
76 randomized in cages, but each cage was randomly assigned to a treatment group. Mice were
77 culled by asphyxiation in a rising concentration of CO₂. Experiments were performed in
78 accordance with the United Kingdom Animals (Scientific Procedures) Act of 1986 (project
79 license number 70/8547).

80 *N. brasiliensis* infection

81 *Nb* was maintained by serial passage through Sprague-Dawley rats, as described¹⁵. Third-stage
82 larvae (L3) were washed ten times with PBS (Dulbecco's PBS, Sigma) before infection. On
83 day 0, mice were infected subcutaneously with 250 larvae (L3). At various time points mice
84 were euthanized and lungs were taken for further analysis.

85 **Flow cytometry**

86 Single-cell suspensions of the lung were prepared for flow cytometry as previously described⁷.
87 For intracellular staining of IL-33 (clone: 396118, Invitrogen) by epithelial cell adhesion
88 molecule (EpCAM) positive cells, a previously described protocol was used¹⁶. Cells were
89 stimulated for 4 h at 37 °C with cell stimulation cocktail containing protein transport
90 inhibitor (eBioscience), then stained with live/dead (Thermo Fisher Scientific). After surface
91 antibody staining, cells were fixed for o/n at 4° C using ICC Fixation buffer (eBioscience),
92 then incubated for 20min at RT in permeabilization buffer (eBioscience). Intracellular
93 staining was performed for IL-33 for 30min at RT. Samples were acquired with an LSR
94 Fortessa II flow cytometer and data analysed using FlowJo software.

95 **Histology and Immunofluorescence**

96 For histology, lungs were inflated with installation of 10% neutral-buffered formalin (NBF;
97 Sigma) and the left lobe of the lung was isolated following *Nb* infection and submersion fixed
98 in NBF. Whole left lung lobes were processed using a tissue processor (Leica ASP300S) and
99 embedded in paraffin. Paraffin blocks were then sectioned to 5 µm using a microtome (Leica
100 RM2235). For immunostaining, lung sections were deparaffinised, rehydrated and heat-
101 mediated antigen retrieval using 10mM sodium citrate buffer (pH 6.0) was performed. To block
102 non-specific protein-binding, 10% donkey serum was used. Sections were stained using an IL-
103 33 antibody (ab118503, Abcam) 1:1000 diluted in PBS followed by a secondary fluorochrome
104 anti-rabbit NorthernLights NL637-conjugated antibody (NL005; R&D systems, 1:200).
105 Sections were then mounted with Fluormount G containing DAPI (Southern Biotech). Staining
106 was visualised on an EVOS™ FL Imaging System (ThermoFisher Scientific) and fluorescence
107 intensity was calculated with ImageJ software (version 1.44) as described before¹⁷. For all

108 images background was subtracted, then images were brightened to a minimum threshold. IL-
109 33-KO mice, which were kindly provided by Dr. John Grainger (Lydia Becker Institute,
110 Manchester, UK) were used to validate specificity of antibody staining.

111 Neutrophil depletion

112 Neutrophil depletion was performed as described before⁷. In short, mice were injected
113 intraperitoneally with 500 µg of neutrophil depleting antibody (clone 1A8, BioXcell) days -1
114 and 1 post infection. Control mice were treated with a corresponding isotype control (IgG2a).

115 IL-33 inhibition

116 IL-33 was suppressed using *Heligmosomoides polygyrus* alarmin release inhibitor (HpARI).
117 HpARI was generated as previously described¹⁸. HpARI (10µg) was administered intranasally
118 in 30 µl of PBS on day 0 and day 1 post infection with *Nb*. Controls were treated with 30 µl
119 PBS intranasally.

120 mRNA quantification

121 RNA extraction and quantitative rtPCR was performed as previously described⁷. The
122 expression of *Il33* mRNA was normalized to that of the housekeeping gene *Actb* (β-actin).

123 IL-33 ELISA

124 Bronchoalveolar lavage (BAL) was performed using 10% FBS in PBS. Collected BAL fluid
125 was centrifuged at 400g for 5min to pellet the cells, and supernatants collected. IL-33
126 concentrations were measured by ELISA (IL-33 duoset, R&D systems) and detected using
127 horseradish peroxidase-conjugated streptavidin and TMB substrate (Biolegend) and the
128 reaction stopped with H₂SO₄. Absorbance was measured at 450nm using a VersaMax
129 microplate reader (Molecular Devices).

130 Statistics

131 Prism 7.0 (version 7.0c, GraphPad Software) was used for statistical analysis. Differences
132 between experimental groups were assessed by Kruskal-Wallis test for nonparametric data,
133 followed by Dunn's multiple comparisons test. For gene expression data, values were log2
134 transformed to achieve normal distribution. Comparisons with a P value < 0.05 were considered
135 to be statistically significant. Data are represented as mean ± sem.

136

137 **Results & Discussion**

138 **Lack of IL-17A leads to impaired early IL-33 production during *Nb* infection**

139 IL-33 is a key alarmin strongly associated with type 2 immunity¹⁹. Both IL-33 and its receptor
140 ST2 have been shown to be implemented in the defense against different nematode infections
141 including *Nb*¹³, *Litomosoides sigmodontis*²⁰ and *Strongyloides ratti*³. We recently described
142 IL-17A as an important initiator of type 2 responses in the lung by downregulating early IFN γ
143 production⁷. To investigate the relationship between IL-17A and IL-33 during the early phase
144 of infection, both *Il17a*-KO and WT mice were infected with 250 L3 *Nb* larvae and the
145 pulmonary immune response assessed at d1 and d2pi. Using flow cytometry, we found that
146 infection driven IL-33 was produced by EpCAM $^+$ CD45 $^-$ lung epithelial cells (Fig. 1A). A
147 comparison between WT and *Il17a*-KO mice demonstrated a significant reduction in IL-33
148 production by EpCAM $^+$ CD45 $^-$ cells in *Il17a*-KO mice compared to WT controls ((Fig. 1B)). IL-
149 33 expression was detected in the lung epithelium early during infection at 16h (Fig. 1C),
150 possibly correlating with the time point *Nb* larvae enter the lung. Using ELISA, we determined
151 that by 24h post infection WT mice secreted significantly higher amounts of IL-33 into the
152 bronchoalveolar lavage fluid (BAL) compared to infected *Il17a*-KO mice (Fig. 1D). Taken
153 together, these data reveal an IL-33 regulating function of IL-17A during the early stages of *Nb*
154 infection.

155 To further identify localization of IL-33 production during *Nb* infection, we examined
156 immunofluorescence staining in lung sections from d1 infected WT and *Il17a*-KO mice. IL-33
157 expression was detected in lungs of both, naïve WT and *Il17a*-KO mice (Fig. 1E). However,
158 consistent with the flow cytometry data the bronchial epithelial cell staining for IL-33 was less
159 intense in *Nb* infected *Il17a*-KO mice, relative to the infected WT mice (Fig. 1E). In accordance
160 with the observations of Hung et al.¹³, quantification of the IL-33 positive areas of the lung
161 airways revealed a significant increase in IL-33 intensity between naïve and d1 infected WT
162 mice (Fig. 1F). However, we observed significantly lower IL-33 intensity in the airways of
163 *Il17a*-KO mice (Fig. 1F). In fact, *Il17a*-KO mice failed to upregulate IL-33 in the bronchial
164 epithelium after *Nb* infection. In contrast to the bronchial epithelium, IL-33 expression by the
165 cells in the lung parenchyma, did not differ between genotypes at the same time point. IL-33
166 intensity in the lung parenchyma was quantified, but we did not observe any statistical
167 differences between all tested groups (Fig. 1G). Due to previous reports^{16,22}, we investigated
168 the possibility that myeloid cells were the source of IL-33 expression in the lung parenchyma
169 by co-staining lung sections for both IL-33 and Ym1. Ym1 is a chitinase-like protein known to
170 induce IL-17A and thereby promote pulmonary type 2 responses⁸. In the lung, Ym1 is mainly
171 expressed by myeloid cells including macrophages and neutrophils^{23,24}. Lung sections stained
172 for both Ym1 (pink) and IL-33 (yellow) revealed no co-staining, suggesting that the source of
173 IL-33 in the parenchyma was not myeloid cells (Fig. 1H). The lung epithelium is a major barrier
174 surface and is known to respond to IL-17A by producing antimicrobial proteins or neutrophil
175 chemoattractants²⁵. As such, lung-epithelial specific deletion of IL-17RA results in impaired
176 clearance of *Klebsiella pneumoniae* infection²⁶. Our finding that during early *Nb* infection, the
177 presence of IL-17A leads to increased airway epithelial derived-IL-33, along with other recent
178 studies⁹ suggest that IL-17A regulation of lung epithelium extends beyond the induction of

179 proinflammatory and anti-microbial factors, and involves regulation of type 2-associated
180 molecules.

181 The molecule Ym1 is responsible for early IL-17A production during *Nb* infection⁸, and thus
182 an early type 2 ‘trigger’ may be needed for IL-17A to promote type 2 responses. The early
183 Ym1 needed to induce IL-17A and promote type 2 immunity, is mostly IL-4R α independent²³
184 but as infection progresses Ym1 production becomes increasingly IL-4R α -dependent, and
185 functions to repair lung damage, in part through the induction of RELM α by lung epithelial
186 cells²³. At this stage, when the type 2 immune response is fully established, the role of IL-17A
187 switches to suppress rather than enhance the type 2 immune response. Whether IL-17A
188 regulation of IL-33 also differs during the early versus later adaptive stages of infection is
189 unknown, but Hung et al have demonstrated that the context and cell source of IL-33 impacts
190 its role in anti-helminth immunity²². Thus, it is important to understand the specific
191 consequence of epithelial cell-derived IL-33. A possible mechanism by which IL-17A induces
192 IL-33 is suggested by work on human epidermal keratinocytes, where IL-17A causes
193 phosphorylation of EGFR, ERK, p38 and STAT1, which is necessary for the induction of IL-
194 33²⁷.

195 **Suppressing IL-33 during *Nb* infection does not increase IFN γ production.**

196 We have reported that during *Nb* infection, early IL-17A is responsible for the suppression of
197 IFN γ from all cellular sources⁷. Here we observed that in the absence of IL-17A IL-33
198 expression in the lung epithelium and IL-33 secretion into the BAL fluid is reduced. We
199 therefore asked whether the ability of IL-17A to limit IFN γ production is acting indirectly
200 through promotion of IL-33. To answer this question we used a known suppressor of IL-33, the
201 *H.polygyrus*-derived protein HpARI, previously shown to inhibit type 2 immune response
202 during *Nb* infection¹⁸. HpARI directly binds to IL-33 and nuclear DNA, blocking the interaction
203 of IL-33 with the ST2 receptor¹⁸. Furthermore, HpARI prevents release of IL-33 from necrotic
204 cells¹⁸. HpARI was administered intranasally at d0 and d1 of *Nb* infection and IFN γ production
205 was investigated d2pi (Fig. 2A). Consistent with our previous findings⁷, at d2pi there was a
206 significant decrease in the proportion of CD8+ T cells (Fig. 2B), $\gamma\delta$ T cells, and NK cells
207 producing IFN γ (Fig. 2B-E). Notably, blocking IL-33 with HpARI in *Nb* infected mice did not
208 reverse the suppression of IFN γ (Fig. 2 B-E). In contrast and as expected, *Il17a*-KO mice
209 exhibited significantly increased IFN γ production compared to WT controls at d2pi with *Nb*.
210 To validate that HpARI treatment was successfully blocking IL-33, we analyzed the numbers
211 of ILC2s in the lung and observed a significant reduction in IL-5+ILC2s in the lung at d2pi
212 (Fig. 2F) further confirming the requirement for IL-33 in type 2 mediated immunity during *Nb*
213 infection¹³. Additionally, IL-33 protein levels in lung homogenates were significantly reduced
214 after HpARI treatment (Fig. 2G). In summary, the evidence does not support a role for IL-33
215 in the suppression of IFN γ during the early stages of pulmonary nematode infection. Because
216 blocking IFN γ rescues type 2 immunity in *Il17a*-KO mice⁷ the suppression of IFN γ by IL-17A
217 is sufficient to initiate type 2 responses, without the need to enhance IL-33 expression. The data
218 therefore suggests that IL-17A induction of type 2 responses involves two fully independent
219 pathways, suppressing IFN γ by lymphocytes and promoting IL-33 production by lung airway

220 epithelial cells. However, a likely consequence of incoming L3 larvae is IL-33 release by
221 damaged epithelial cells, which raises the question as to what are the circumstances that require
222 IL-17A to further enhance IL-33 expression. A better understanding of the connection between
223 IL-33 and IFN γ in this setting is therefore needed.

224 **IL-17A-dependent neutrophilia is not a driver of IL-33 production**

225 A hallmark characteristic of IL-17A is its ability to promote neutrophil recruitment⁸. During
226 the early phases of *Nb* infection, neutrophils are rapidly recruited to the lungs, with peak-
227 neutrophilia being between d1 and d2pi²⁸. Neutrophils primed by *Nb* infection have been shown
228 to upregulate *Il33* transcripts²⁸ and are a major driver of tissue injury which in turn could lead
229 to IL-33 release. Therefore, we investigated whether neutrophils recruited during *Nb* infection
230 contribute to IL-33 levels in the lung. Neutrophils were depleted at d-1 and 1pi (Fig. 3A) and
231 successful depletion was confirmed via flow cytometry. Injection of anti-Ly6G effectively
232 prevented neutrophil accumulation in the BAL at d2pi compared to isotype control (Fig. 3B).
233 Histological sections of the lungs demonstrated infection-induced injury at d2pi in isotype-
234 treated WT mice, an effect that is almost absent in infected mice depleted of neutrophils (Fig.
235 3C). Using measures of lacunarity as an indicator of acute lung injury²⁹, neutrophil depleted
236 mice displayed no significant signs of damage (Fig. 3C). These findings reinforce previous
237 observations that neutrophilia is largely responsible for the severe lung damage observed in this
238 model²⁸. To investigate whether this extensive tissue damage during the early stage of *Nb*
239 infection could be responsible for the increase in IL-33 release, lung sections were stained for
240 IL-33 (Fig. 3D). Quantification of the IL-33 positive areas in the lung airways as well as the
241 lung parenchyma did not reveal a difference between mice depleted of neutrophils and isotype
242 controls (Fig. 3E, F). While infected mice exhibited increased IL-33 intensity compared to
243 naïve mice, no significant difference was observed between the treatment groups. If neutrophils
244 are a contributor of IL-33 during *Nb* infection, we would have expected less IL-33 after
245 depleting the peak neutrophilia. However, mice depleted of neutrophils had a slightly higher
246 intensity for epithelial IL-33 staining at d2pi, although this difference did not reach statistical
247 significance (Fig. 3F). Depleting neutrophils also did not change the IL-33 levels at later stage
248 of *Nb* infection as shown for d6pi in both lung epithelium and lung parenchyma (Fig. 3E, F).
249 Our data therefore demonstrate that during the lung-migrating phase of *Nb* infection,
250 neutrophil-mediated damage is not the cause of IL-33 production.

251 In summary, our brief report further implicates pulmonary IL-17A in the initiation phase of
252 type 2 immunity in the lung. Through two independent mechanisms, enhanced IL-33
253 production by the lung epithelium, and suppression of IFN γ , IL-17A supports the type 2
254 immune response in the lung needed to cope with lung-migrating helminth infection.

255 **Acknowledgments**

256 We thank the Flow Cytometry, Bioimaging, and Biological Services core facilities at the
257 University of Manchester. This work was supported by the Wellcome Trust (106898/A/15/Z to
258 JEA) with additional support from the Medical Research Council UK (MR/K01207X/1 to JEA)
259 and the Wellcome Trust (221914/Z/20/Z to HJM)

260 **Author Contribution**

261 J.A. executed experiments, S.P., J.E.P., and B.H.K.C. provided experimental assistance. J.A.,
262 T.E.S., J.E.A. designed experiments and analysed data, H.J.M. provided reagents and
263 experimental advice. J.A., T.E.S. and J.E.A. wrote the original draft of the manuscript and all
264 co-authors reviewed and edited the manuscript.

265 **Disclosures**

266 The authors have no financial conflicts of interest.

267

- 268 1. Cayrol, C. & Girard, J. P. Interleukin-33 (IL-33): A nuclear cytokine from the IL-1
269 family. *Immunological Reviews* vol. 281 154–168 (2018).
- 270 2. Molofsky, A. B., Savage, A. K. & Locksley, R. M. Interleukin-33 in Tissue
271 Homeostasis, Injury, and Inflammation. *Immunity* vol. 42 1005–1019 (2015).
- 272 3. Moussion, C., Ortega, N. & Girard, J. P. The IL-1-like cytokine IL-33 is constitutively
273 expressed in the nucleus of endothelial cells and epithelial cells in vivo: A novel
274 ‘Alarmin’? *PLoS One* **3**, (2008).
- 275 4. Yasuda, K. *et al.* Contribution of IL-33-activated type II innate lymphoid cells to
276 pulmonary eosinophilia in intestinal nematode-infected mice. *Proc. Natl. Acad. Sci. U.*
277 *S. A.* **109**, 3451–3456 (2012).
- 278 5. Kouzaki, H., Iijima, K., Kobayashi, T., O’Grady, S. M. & Kita, H. The Danger Signal,
279 Extracellular ATP, Is a Sensor for an Airborne Allergen and Triggers IL-33 Release
280 and Innate Th2-Type Responses. *J. Immunol.* **186**, 4375–4387 (2011).
- 281 6. Mills, K. H. G. IL-17 and IL-17-producing cells in protection versus pathology. *Nat.*
282 *Rev. Immunol.* (2022) doi:10.1038/S41577-022-00746-9.
- 283 7. Ajendra, J. *et al.* IL-17A both initiates, via IFN γ suppression, and limits the pulmonary
284 type-2 immune response to nematode infection. *Mucosal Immunol.* **13**, 958–968
285 (2020).
- 286 8. Sutherland, T. E. *et al.* Chitinase-like proteins promote IL-17-mediated neutrophilia in
287 a tradeoff between nematode killing and host damage. *Nat. Immunol.* (2014)
288 doi:10.1038/ni.3023.
- 289 9. Guo, X. zhi J. *et al.* Lung $\gamma\delta$ T Cells Mediate Protective Responses during Neonatal
290 Influenza Infection that Are Associated with Type 2 Immunity. *Immunity* **49**, 531–
291 544.e6 (2018).
- 292 10. Kohlgruber, A. C. *et al.* $\gamma\delta$ T cells producing interleukin-17A regulate adipose
293 regulatory T cell homeostasis and thermogenesis /631/250/256 /631/250/2504 article.
294 *Nat. Immunol.* **19**, 464–474 (2018).
- 295 11. Kim, M. H. *et al.* IL-17A-Producing Innate Lymphoid Cells Promote Skin
296 Inflammation by Inducing IL-33-Driven Type 2 Immune Responses. *J. Invest.*
297 *Dermatol.* **140**, 827-837.e9 (2020).
- 298 12. Garth, J. M. *et al.* IL-33 Signaling Regulates Innate IL-17A and IL-22 Production via
299 Suppression of Prostaglandin E 2 during Lung Fungal Infection . *J. Immunol.* **199**,
300 2140–2148 (2017).

301 13. Hung, L.-Y. *et al.* IL-33 drives biphasic IL-13 production for noncanonical Type 2
302 immunity against hookworms. *Proc. Natl. Acad. Sci. U. S. A.* **110**, 282–7 (2013).

303 14. Srinivas, S. *et al.* Cre reporter strains produced by targeted insertion of EYFP and
304 ECFP into the ROSA26 locus. *BMC Dev. Biol.* **1**, 1–8 (2001).

305 15. Lawrence, R. A., Gray, C. A., Osborne, J. & Maizels, R. M. *Nippostrongylus*
306 *brasiliensis*: Cytokine responses and nematode expulsion in normal and IL-4 deficient
307 mice. *Exp. Parasitol.* **84**, 65–73 (1996).

308 16. Wills-Karp, M. *et al.* Trefoil factor 2 rapidly induces interleukin 33 to promote type 2
309 immunity during allergic asthma and hookworm infection. *J. Exp. Med.* **209**, 607–622
310 (2012).

311 17. Chinery, A. L. *et al.* IL-13 deficiency exacerbates lung damage and impairs epithelial-
312 derived type 2 molecules during nematode infection. *Life Sci. Alliance* **4**, e202001000
313 (2021).

314 18. Osbourn, M. *et al.* HpARI Protein Secreted by a Helminth Parasite Suppresses
315 Interleukin-33. *Immunity* **47**, 739-751.e5 (2017).

316 19. Drake, L. Y. & Kita, H. IL-33: biological properties, functions, and roles in airway
317 disease. *Immunological Reviews* vol. 278 173–184 (2017).

318 20. Ajendra, J. *et al.* ST2 deficiency does not impair type 2 immune responses during
319 chronic filarial infection but leads to an increased microfilaremia due to an impaired
320 splenic microfilarial clearance. *PLoS One* **9**, (2014).

321 21. Meiners, J. *et al.* IL-33 facilitates rapid expulsion of the parasitic nematode
322 *Strongyloides ratti* from the intestine via ILC2- And IL-9-driven mast cell activation.
323 *PLoS Pathog.* **16**, (2020).

324 22. Hung, L. Y. *et al.* Cellular context of IL-33 expression dictates impact on anti-helminth
325 immunity. *Sci. Immunol.* **5**, (2020).

326 23. Sutherland, T. E. *et al.* Ym1 induces RELM α and rescues IL-4R α deficiency in lung
327 repair during nematode infection. *PLoS Pathog.* **14**, (2018).

328 24. Parkinson, J. E., Pearson, S., Rückerl, D., Allen, J. E. & Sutherland, T. E. The
329 magnitude of airway remodeling is not altered by distinct allergic inflammatory
330 responses in BALB/c versus C57BL/6 mice but matrix composition differs. *Immunol.*
331 *Cell Biol.* **99**, 640–655 (2021).

332 25. Aujla, S. J., Dubin, P. J. & Kolls, J. K. Interleukin-17 in pulmonary host defense. in
333 *Experimental Lung Research* vol. 33 507–518 (2007).

334 26. Chen, K. *et al.* IL-17 Receptor Signaling in the Lung Epithelium Is Required for
335 Mucosal Chemokine Gradients and Pulmonary Host Defense against *K. pneumoniae*.
336 *Cell Host Microbe* **20**, 596–605 (2016).

337 27. Meephansan, J. *et al.* Expression of IL-33 in the epidermis: The mechanism of
338 induction by IL-17. *J. Dermatol. Sci.* **71**, 107–114 (2013).

339 28. Chen, F. *et al.* Neutrophils prime a long-lived effector macrophage phenotype that
340 mediates accelerated helminth expulsion. *Nat. Immunol.* **15**, 938–46 (2014).

341 29. Chinery, A. L. *et al.* Inflammasome-Independent Role for NLRP3 in Controlling
342 Innate Antihelminth Immunity and Tissue Repair in the Lung. *J. Immunol.* **203**, 2724–
343 2734 (2019).

344

345

346 Figure 1:

347 Mice were infected with 250L3 larvae *Nb* and IL-33 production was assessed using different
348 techniques. Representative flow cytometry gating strategy showing intracellular IL-33 for
349 infected mice. Whole lung cells were gated on single and live cells, then for Epcam+CD45-
350 lung epithelial cells (A). Frequency of intracellular IL-33 in Epcam+CD45- lung epithelial
351 cells in WT and *Il17a*-KO mice d2pi (B) and 16h and 40h post *Nb* infection (C). IL-33 in
352 BAL fluid of naïve and mice 24h post infection (D). Microscopy images of
353 immunofluorescent staining for IL-33 (white) in lung sections of WT and *Il17a*- KO mice
354 1d post *Nb* infection and naïve controls (E). Quantification for IL-33 positive areas for lung
355 epithelium (F) and lung parenchyma (G). Antibody positive staining area was quantified
356 for the intensity normalized to background staining. Immunofluorescent staining for Ym1
357 (pink) and IL-33 (yellow) in lung sections of WT mice to confirm co-staining (H). Data are
358 expressed as mean \pm s.e.m. and are representative for 2 individual experiments and were
359 analysed by ANOVA with Tukey's multiple comparison test. * $P < 0.05$, ** $P < 0.01$.

360

361 Figure 2:

362 Mice were infected with 250 L3 larvae *Nb* and either treated with intranasal HpARI or PBS
363 (A). Cellular sources of IFN γ were analysed via flow cytometry. Flow plots of IFN γ
364 production by live TCR β +CD8+ T cells in all tested groups as well as fluorescence minus
365 one (FMO) control (B). Frequency of intracellular IFN γ by $\gamma\delta$ T cells (C), CD8+ T cells
366 (D), and NK cells (E) in naïve mice and mice infected with *Nb* d2pi, either treated with
367 intranasal HpARI or PBS. *Il17a*-KO mice were used as positive controls. Absolute count
368 of IL5+ILC2 in the lung in naïve and *Nb* infected mice (F). IL-33 in BAL fluid of naïve and
369 mice d2pi as quantified via ELISA (G). Data are expressed as mean \pm s.e.m. and are
370 representative for 3 individual experiments and were analysed by ANOVA with Tukey's
371 multiple comparison test. * $P < 0.05$, ** $P < 0.01$.

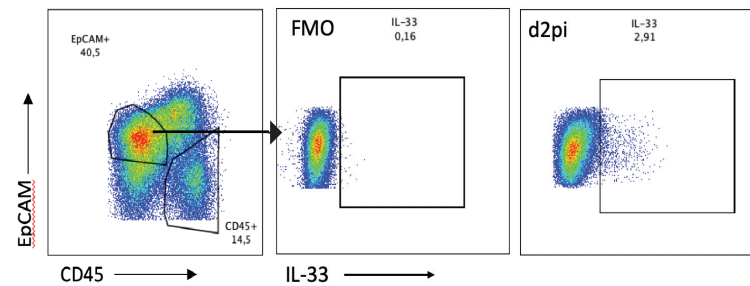
372

373 Figure 3:

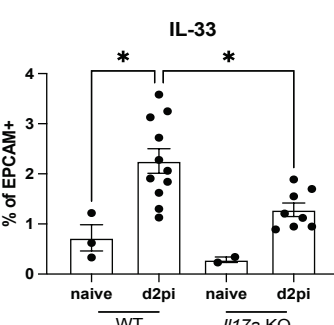
374 C57BL/6J mice were infected with 250 *Nb* L3 larvae and mice were injected
375 intraperitoneally with α -Ly6G (1A8) or corresponding isotype control on d-1 and d1pi and
376 immune responses were measured on d2pi or d6pi compared uninfected naïve mice (A).
377 Confirmation of neutrophil (Gr1 $^+$ CD11b $^+$) depletion via representative flow cytometry
378 plots as well as neutrophil frequency in the BAL (B). Representative images of lung sections
379 stained with hematoxylin & eosin and quantification of lacunarity (Λ) on d2pi and d6pi with
380 *Nb* compared to lungs from uninfected naïve mice (C). Microscopy images of
381 immunofluorescent staining for IL-33 (purple) in lung sections of mice depleted by
382 neutrophils or isotype controls (D). Quantification for IL-33 positive areas for lung
383 epithelium (E) and lung parenchyma (F). Antibody positive staining area was quantified for
384 the intensity normalized to background staining. Data are expressed as mean \pm s.e.m. and
385 are pooled from 2 individual experiments and were analysed by ANOVA with Tukey's
386 multiple comparison test.

387

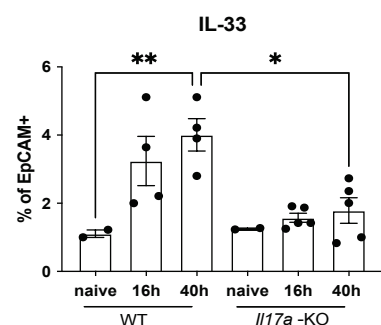
A



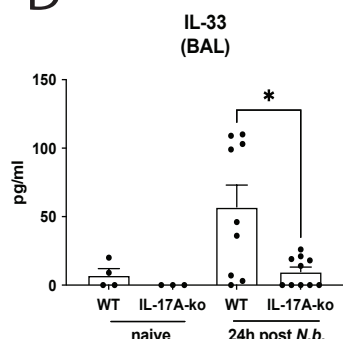
B



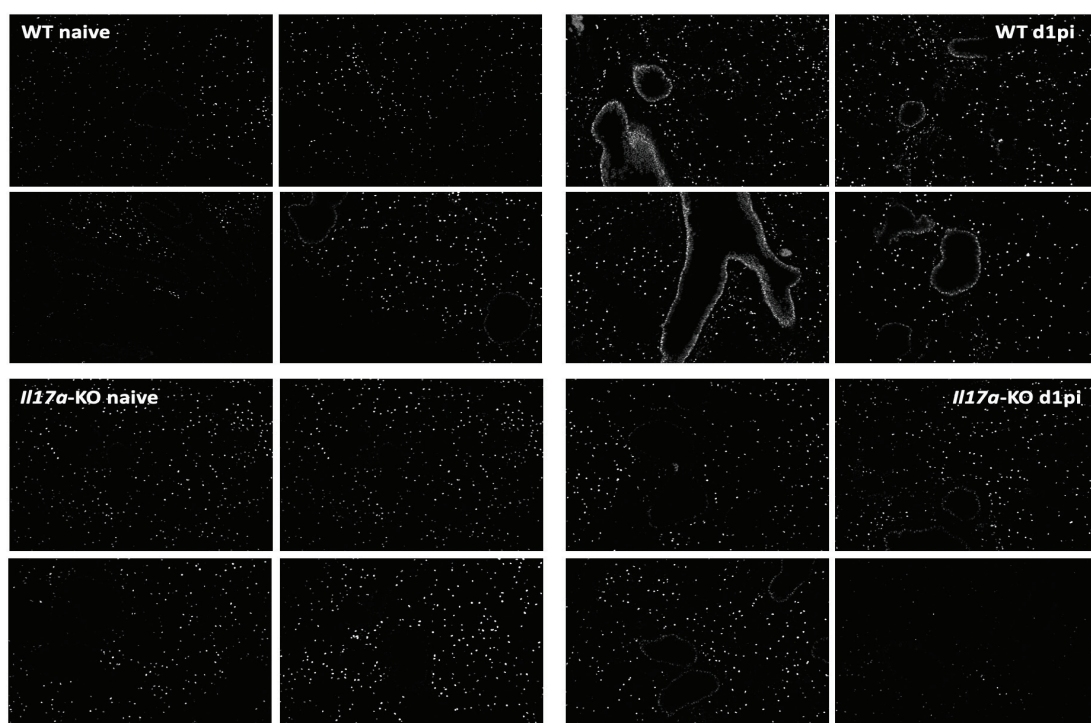
C



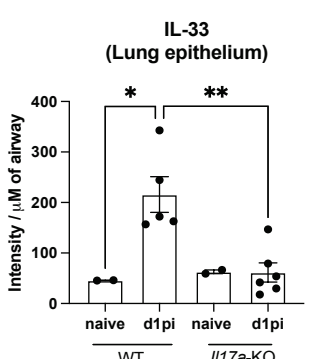
D



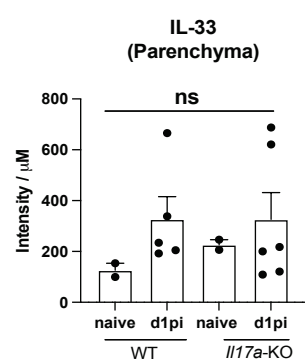
E



F



G



H

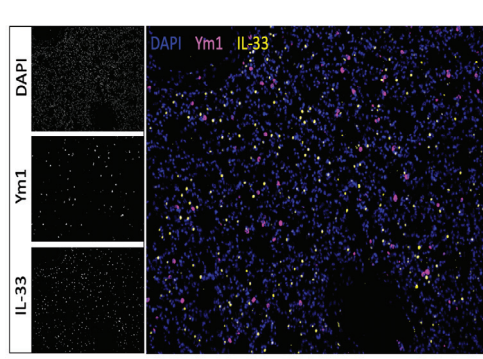
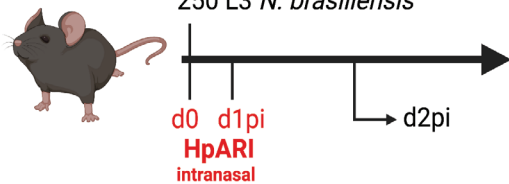


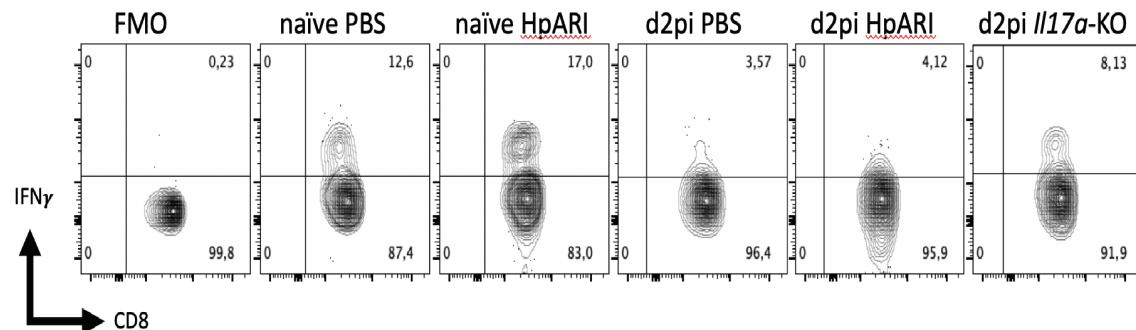
Figure 1

A

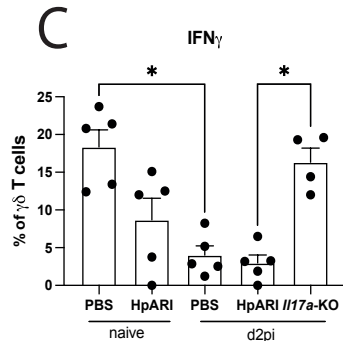
bioRxiv preprint doi: <https://doi.org/10.1101/2022.11.03.515050>; this version posted November 4, 2022. The copyright holder for this preprint (which was not certified by peer review) is the author/funder, who has granted bioRxiv a license to display the preprint in perpetuity. It is made available under aCC-BY-NC-ND 4.0 International license.



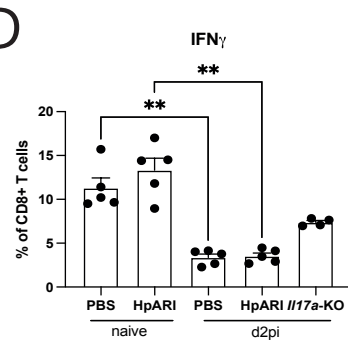
B



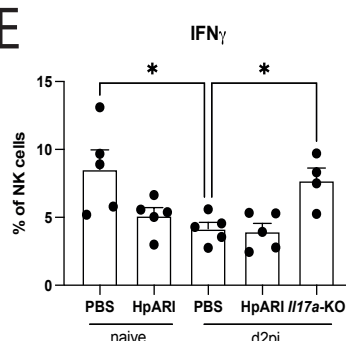
C



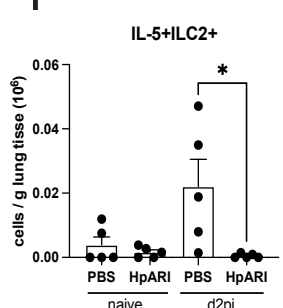
D



E



F



G

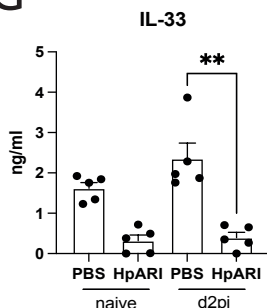
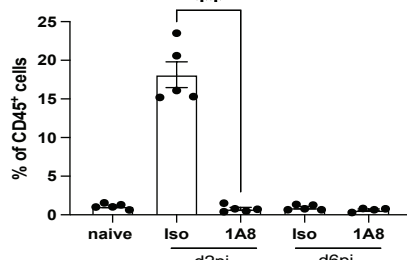
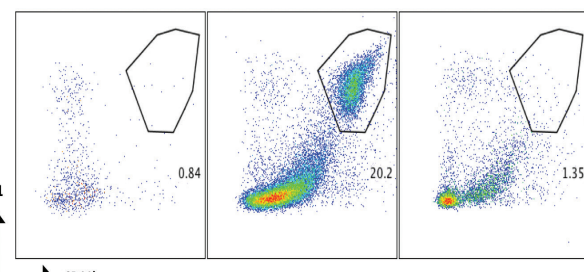
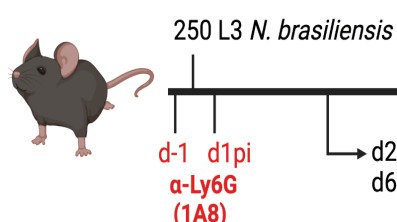


Figure 2

A

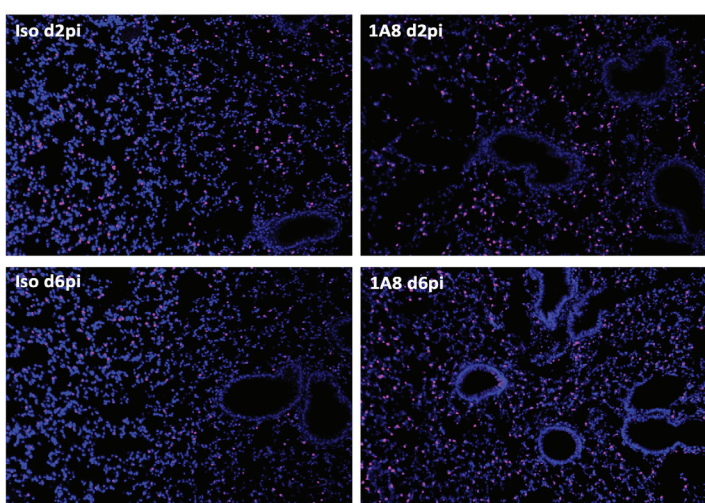


naive

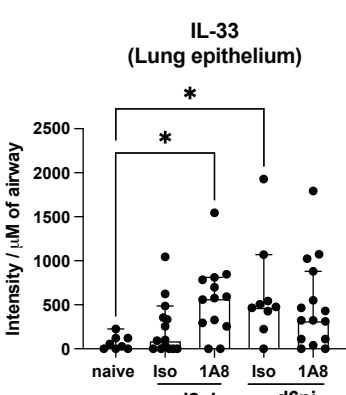
N. brasiliensis d2pi (isotype)

N. brasiliensis d2pi (1A8)

C



E



F

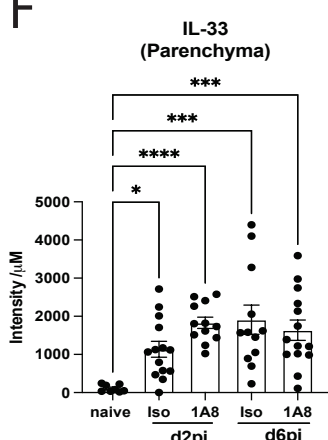


Figure 3